







# NsiR3, a nitrogen stress-inducible small RNA, regulates proline oxidase expression in the cyanobacterium *Nostoc* sp. PCC 7120

Isidro Álvarez-Escribano<sup>1</sup>, Manuel Brenes-Álvarez<sup>1</sup> , Elvira Olmedo-Verd<sup>1</sup> , Jens Georg<sup>2</sup> , Wolfgang R. Hess<sup>2</sup> , Agustín Vioque<sup>1</sup>  and Alicia M. Muro-Pastor<sup>1</sup> 

<sup>1</sup> Instituto de Bioquímica Vegetal y Fotosíntesis, Consejo Superior de Investigaciones Científicas and Universidad de Sevilla, Sevilla, Spain

<sup>2</sup> Genetics and Experimental Bioinformatics, Faculty of Biology, University of Freiburg, Freiburg, Germany

## Keywords

heterocyst; NtcA; post-transcriptional regulation; PutA; regulatory RNA

## Correspondence

A. Vioque, Instituto de Bioquímica Vegetal y Fotosíntesis, Consejo Superior de Investigaciones Científicas and Universidad de Sevilla, Avda. Américo Vespucio 49, Sevilla 41092, Spain  
 Tel: +34-954489519  
 E-mail: vioque@us.es

(Received 14 May 2020, revised 17 July 2020, accepted 10 August 2020)

doi:10.1111/febs.15516

NsiR3 (nitrogen stress-inducible RNA 3) is a small noncoding RNA strongly conserved in heterocyst-forming cyanobacteria. In *Nostoc* sp. PCC 7120, transcription of NsiR3 is induced by nitrogen starvation and depends on the global nitrogen regulator NtcA. A conserved NtcA-binding site is centered around position −42.5 with respect to the transcription start site of NsiR3 homologs, and NtcA binds *in vitro* to a DNA fragment containing this sequence. In the absence of combined nitrogen, NsiR3 expression is induced in all cells along the *Nostoc* filament but much more strongly in heterocysts, differentiated cells devoted to nitrogen fixation. Co-expression analysis of transcriptomic data obtained from microarrays hybridized with RNA obtained from *Nostoc* wild-type or mutant strains grown in the presence of ammonium or in the absence of combined nitrogen revealed that the expression profile of gene *putA* (proline oxidase) correlates negatively with that of NsiR3. Using a heterologous system in *Escherichia coli*, we show that NsiR3 binds to the 5'-UTR of *putA* mRNA, resulting in reduced expression of a reporter gene. Overexpression of NsiR3 in *Nostoc* resulted in strong reduction of *putA* mRNA accumulation, further supporting the negative regulation of *putA* by NsiR3. The higher expression of NsiR3 in heterocysts *versus* vegetative cells of the N<sub>2</sub>-fixing filament could contribute to the previously described absence of *putA* mRNA and of the catabolic pathway to produce glutamate from arginine via proline specifically in heterocysts. Post-transcriptional regulation by NsiR3 represents an indirect NtcA-operated regulatory mechanism of *putA* expression.

## Database

Microarray data are available in GEO database under accession numbers [GSE120377](#) and [GSE150191](#).

## Introduction

In some filamentous cyanobacteria, the acclimation to nitrogen deficiency involves differentiation of heterocysts, a cell type specialized for the fixation of

atmospheric nitrogen [1]. Growth at the expense of N<sub>2</sub> involves complete metabolic remodeling so that two different cell types with different metabolic capabilities

## Abbreviations

2-OG, 2-oxoglutarate; dRNASeq, differential RNA sequencing; FC, fold change; GEO, Gene Expression Omnibus; GOGAT, glutamine oxoglutarate aminotransferase; GS, glutamine synthetase; GSA, glutamate  $\gamma$ -semialdehyde; LB, Luria Broth; OAA, oxaloacetate; OAC, ornithine–ammonium cycle; P5C,  $\Delta^1$ -pyrroline-5-carboxylate; Sm, streptomycin; Sp, spectinomycin; sRNA, small RNA;  $\beta$ -Asp-Arg,  $\beta$ -aspartylarginine; STRR, short tandemly repeated repetitive; TCA, tricarboxylic acid cycle.

(vegetative cells and heterocysts) cooperate to achieve growth of the filament as a whole [2]. The differentiation of heterocysts involves complex transcriptional changes both in vegetative cells and in heterocysts not only to achieve morphological differentiation of heterocysts but also to undergo metabolic adaptations required for growth at the expense of N<sub>2</sub> [3,4].

Small RNAs (sRNAs) constitute a relevant class of post-transcriptional regulators involved in the adaptation of bacterial metabolism to different environmental situations [5]. sRNAs can coordinate changes in gene expression in response to environmental stresses. Similar to the observations made in other groups of bacteria, cyanobacteria exhibit abundant transcription of non-coding RNAs, including antisense RNAs and sRNAs, and transcription of many of them is regulated in response to nitrogen availability [6–9]. Several nitrogen-regulated noncoding RNAs have been identified and characterized in the filamentous, heterocyst-forming cyanobacterium *Nostoc* sp. PCC 7120 [3,10–14]. Furthermore, heterocyst-specific transcription of noncoding RNAs has been described [3,11,15,16], and some of those transcripts affect the process of heterocyst differentiation [17] or the regulation of enzymatic activities whose levels must be adjusted specifically in heterocysts *versus* vegetative cells [13].

NsiR3 is an sRNA whose expression is induced upon nitrogen deprivation and depends on NtcA, the global nitrogen regulator in cyanobacteria [9,11]. It was originally described as conserved in 27 heterocyst-forming cyanobacteria but absent in nonheterocystous strains [11], suggesting a possible role of NsiR3 related to heterocyst function. However, no regulatory target has so far been identified for NsiR3.

Computational prediction of mRNAs regulated by a given sRNA can be misleading because the interactions between sRNAs and their targets take place through short, often discontinuous complementary sequences [18]. Experimental identification of possible targets based on simple analysis of differences in expression changes upon alteration of the amount of the sRNA is in many cases impeded by secondary effects. Furthermore, such approaches rely on the assumption that the post-transcriptional regulation exerted by the sRNA results in clear changes in the amount of the target mRNA, which is not necessarily true [19]. For this reason, the combination of computational and more sophisticated experimental approaches is often more productive (reviewed in Ref. [20]).

In this work, we show that upon nitrogen deprivation, expression of NsiR3 is more strongly induced in heterocysts than in vegetative cells. By using a novel approach based on correlation of expression analysis

we identify *putA*, that encodes proline oxidase, as a target of NsiR3 because of the strong negative correlation with NsiR3. Finally, we demonstrate the interaction between NsiR3 and the 5'-UTR of the *putA* mRNA, and the negative regulation exerted by NsiR3 on the expression of *putA* in *Nostoc* sp. PCC 7120.

## Results

### NsiR3 is conserved in heterocyst-forming cyanobacteria, and its transcription is induced upon nitrogen stress

The nitrogen-regulated transcription of NsiR3 was discovered in a previous dRNASeq experiment [9]. Phylogenetic conservation of NsiR3 homologs across cyanobacterial genomes was later described [11], and we have now identified NsiR3 homologs in additional cyanobacteria, confirming that NsiR3 appears restricted to heterocyst-forming strains (Fig. 1).

In *Nostoc* sp. PCC 7120, NsiR3 is transcribed downstream of *all4558* and in the opposite orientation (Fig. 2A). The predicted secondary structure contains two possible stem-loops acting as transcriptional terminators (Fig. 2B); the second one (T2) is also found in closely related cyanobacterial strains and is formed by STRR (short tandemly repeated repetitive) imperfect 7-nt repeats that are present in genomes of filamentous cyanobacteria usually in intergenic regions but in some case within coding sequences. Their function, if any, is unknown [21,22] (Fig. 2C). Expression of NsiR3 is induced upon nitrogen stress (Fig. 2D,E). Induction upon removal of combined nitrogen is quick, and the amounts of NsiR3 remain high up to 24 h. Transfer from ammonium-containing medium to nitrate-containing medium also induces NsiR3 expression but to lower levels and the induction is transient (Fig. 2D,E), reflecting the fact that nitrogen stress in these conditions is quickly relieved by derepression of the *nir* operon which encodes nitrate reductase and nitrite reductase, the enzymes involved in assimilation of nitrate [23,24]. Consistent with the predicted secondary structure, two RNAs, of 45 and 115 nucleotides, were detected by northern hybridization with the NsiR3 probe. The 45-nucleotide RNA (NsiR3S) is of the expected size from the experimentally determined transcriptional start site (TSS) for NsiR3 [9] to the first predicted terminator, T1. The major detected band is 115 nucleotides long (NsiR3L) and matches the calculated length from the TSS to the second predicted terminator, T2, further downstream (Fig. 2B). NsiR3L is the most abundant of the two species of NsiR3; therefore, it was used in all the experiments described here.



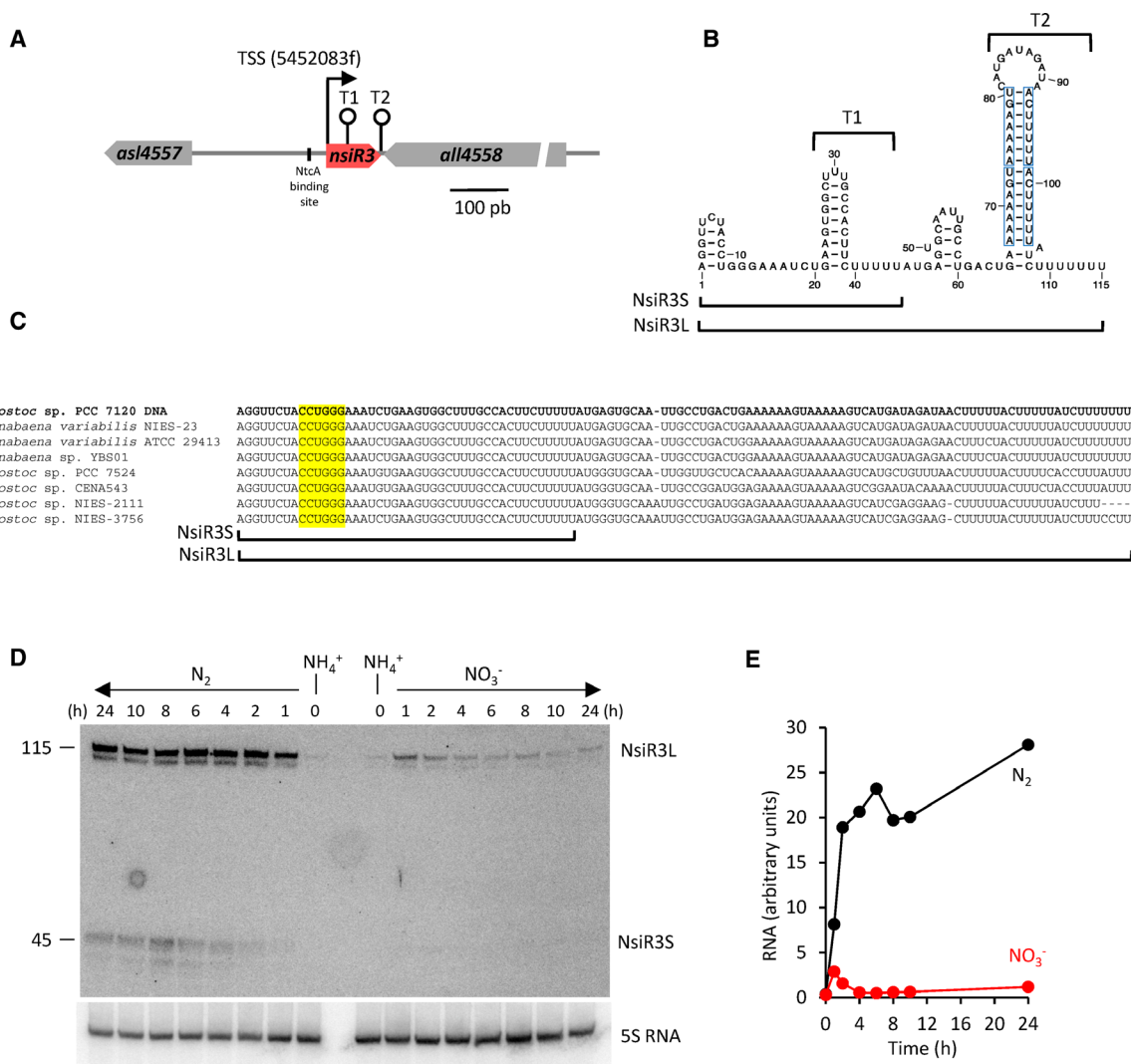


**Fig. 2.** The nitrogen stress-inducible (NsiR3). (A) Schematic representation of the region encoding NsiR3 in *Nostoc* sp. PCC 7120. The two flanking genes are indicated. The bent arrow represents the transcriptional start at position 5452083f, and the stem-loops represent the two transcriptional terminators of NsiR3. The position of the NtcA-binding site is also indicated. (B) Secondary structure model of NsiR3 from *Nostoc* sp. PCC 7120 based on the consensus obtained with RNAalifold from the alignments in Fig. 1 and C this image. The heptanucleotide repeats (STRR) are framed. (C) The sequences of NsiR3 encoded in those strains that could have a second transcriptional terminator (T2) further downstream T1 were aligned using CLUSTAL OMEGA. The predicted seed region is highlighted in yellow. Accession numbers are indicated in Fig. 1. (D) Nitrogen-responsive expression of NsiR3 in *Nostoc* sp. PCC 7120. Expression was analyzed by northern blot in cells grown in the presence of ammonium and transferred to medium containing no source of combined nitrogen ( $N_2$ ) or containing nitrate ( $NO_3^-$ ) for the number of hours indicated. The upper panel shows hybridization to the NsiR3 probe. The lower panel shows hybridization to a probe for 5S RNA used as loading and transfer control. Sizes (nt) are indicated on the left. The experiment was repeated four times with similar results. The northern blot containing the highest number of time points is shown. (E) Quantification of NsiR3L in the blot shown in (D) upon nitrogen removal (black,  $N_2$ ) or upon nitrogen removal followed by nitrate addition (red,  $NO_3^-$ ).

### NtcA directly regulates NsiR3 expression

Transcription of NsiR3 in *Nostoc* sp. PCC 7120 depends on NtcA [9,11]. Alignment of the promoter region from all 70 identified *nsiR3* sequences shows that a putative conserved NtcA-binding sequence

appears centered around position  $-42.5$  in 67 of them (Fig. 3), which is compatible with direct activation of NsiR3 transcription by NtcA.

To verify the interaction between NtcA and the promoter region of *nsiR3*, we performed an electrophoretic mobility shift assay with purified NtcA



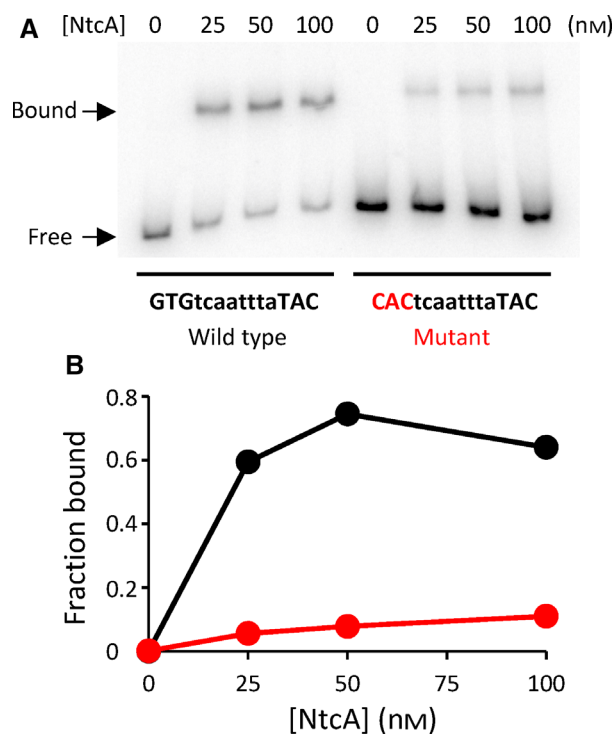


**Fig. 4.** NtcA binds to the *nsiR3* promoter. (A) Electrophoretic mobility shift assays showing binding of purified His-tagged NtcA protein to a DNA fragment containing the wild-type promoter of NsiR3 from *Nostoc* sp. PCC 7120 (left) or a mutated version altered in the positions indicated in red (right). Three times more probe was used in the assay with the mutant fragment than with the wild-type fragment. A representative experiment is shown. (B) Quantification of the autoradiogram presented in panel (A). The fraction of probe bound by NtcA was calculated for the wild-type (black) or the mutated (red) version.

protein and a DNA fragment extending from positions –118 to +31 with respect to the TSS of *nsiR3* that includes the possible NtcA-binding sequence. In the presence of NtcA, a retarded complex was observed with the fragment containing the wild-type promoter sequence (Fig. 4A). However, the fraction of fragment bound by NtcA was strongly (ninefold) reduced (Fig. 4A,B) when the assay was performed with a DNA fragment containing a version of the *nsiR3* promoter with the NtcA-binding site mutated (GTG changed to CAC). These results demonstrate the binding of NtcA to a specific sequence of the *nsiR3* promoter.

#### NsiR3 accumulates differentially in heterocysts but is not essential for diazotrophic growth

It was previously shown that NsiR3 transcription is dependent on NtcA but independent of HetR [9,11], the master regulator of heterocyst differentiation.

Therefore, we expect that NsiR3 transcription would be induced in all cells of the filament upon nitrogen stress. To characterize the pattern of expression of NsiR3, we prepared a plasmid containing a transcriptional fusion of the NsiR3 promoter to the *gfp* gene (pSAM341, see Table S4). The plasmid was introduced in *Nostoc* sp. PCC 7120 by conjugation, and expression of GFP was analyzed by confocal fluorescence microscopy (Fig. 5). Filaments growing in ammonium-containing medium had very low green fluorescence, while filaments growing in medium lacking combined nitrogen showed fluorescence in all cells, but peaks of green fluorescence were associated with cells that were differentiating as heterocysts, as indicated by their lower red autofluorescence. Interestingly, induction of the *nsiR3* promoter occurs early in heterocyst development because significant green fluorescence was already observed in immature heterocysts, still having substantial red fluorescence (not shown).

The conservation of NsiR3 in heterocyst-forming cyanobacteria and its NtcA-dependent expression suggests that NsiR3 is involved in some aspect of the regulation of the response to nitrogen stress in these complex cyanobacteria that includes differentiation of specialized cells. To explore the possible function of NsiR3, we constructed a *Nostoc* strain lacking NsiR3 ( $\Delta$ *nsiR3*). This strain grew similarly to wild-type in media containing ammonium and nitrate, or lacking combined nitrogen (Fig. 6); therefore, the differentiation of functional heterocysts is not compromised in the absence of NsiR3.

#### NsiR3 is a regulator of *putA* (*alr0540*)

Bacterial sRNAs impact their target mRNAs often by repressing the initiation of translation via binding to their 5'-UTRs [5]. Hence, the mRNAs do not associate with ribosomes and may become more vulnerable to ribonucleases, leading to reduced mRNA level. To identify potential targets of NsiR3 whose expression would be negatively regulated by NsiR3 in *Nostoc* sp. PCC 7120, we decided to search for genes whose expression profile showed a negative correlation with the expression of NsiR3. For this purpose, we have used a novel approach based on correlation analysis of data obtained from hybridization of high-density microarrays [3]. In order to identify those genes with negative correlation with NsiR3, we analyzed data obtained from hybridization of RNA samples extracted from the  $\Delta$ *nsiR3* mutant grown in ammonium-containing medium (two replicates) or from the  $\Delta$ *nsiR3* mutant after 8 h of incubation in medium lacking combined nitrogen (two replicates). In addition, in order to increase the

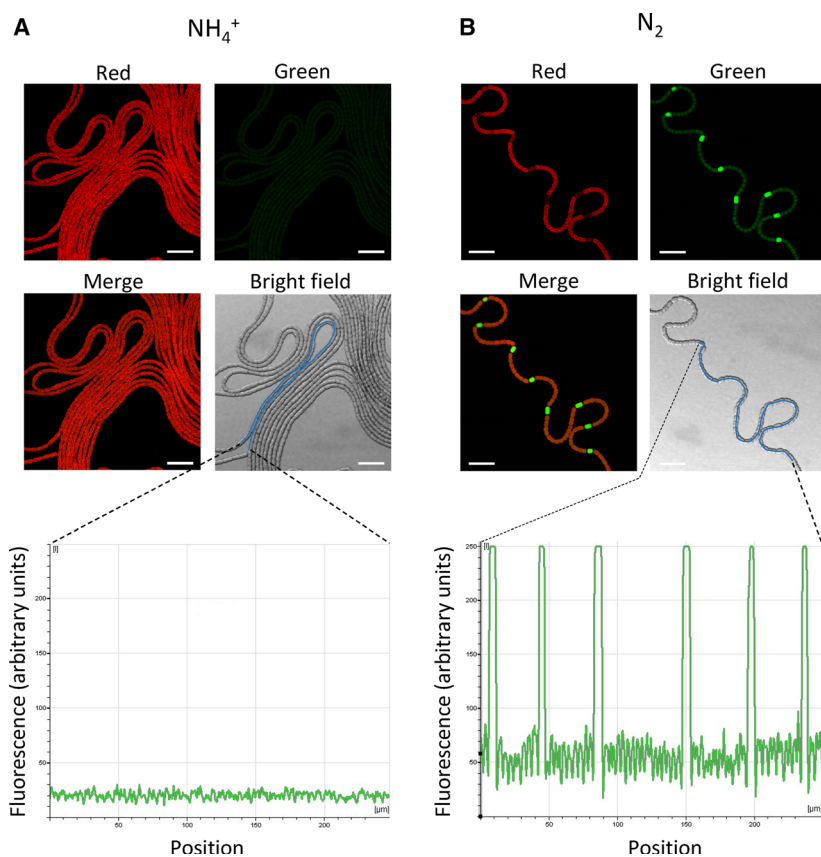


**Fig. 5.** Expression pattern of the *nsiR3* promoter in *Nostoc* filaments. Confocal fluorescence images (red channel, green channel, both channels merged, and bright-field image) of *Nostoc* filaments carrying the *gfp* gene under the control of the *nsiR3* promoter (plasmid pSAM341) and growing on top of medium containing ammonium,  $\text{NH}_4^+$  (A), or lacking any source of combined nitrogen,  $\text{N}_2$  (B). Quantification of the signals for the green channel (GFP) is shown for the segments indicated by a blue line in the corresponding bright-field images. All images were acquired with the same sensitivity settings so that intensities can be compared. Scale bars, 20  $\mu\text{m}$ .

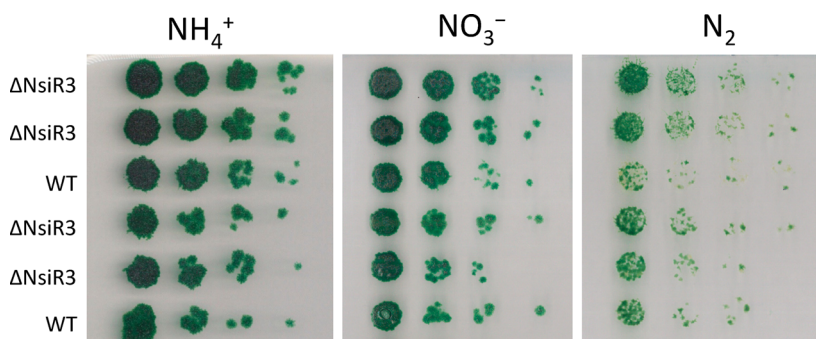


**Fig. 6.** The  $\Delta\text{nsiR3}$  strain can differentiate heterocysts. Cells were grown in the presence of nitrate, washed with  $\text{BG11}_0$ , and resuspended at  $0.1 \mu\text{g chlorophyll}\cdot\text{mL}^{-1}$ . Fivefold serial dilutions of liquid cultures of wild-type or four independent  $\Delta\text{nsiR3}$  isolates were prepared. Ten microlitre of the cell suspension and of three fivefold serial dilutions were plated on  $\text{BG11}_0$  plates containing ammonium ( $\text{NH}_4^+$ ), nitrate ( $\text{NO}_3^-$ ), or no source of combined nitrogen ( $\text{N}_2$ ). Pictures were taken after 10 days of incubation at  $30^\circ\text{C}$ .

sensitivity of the correlation analysis, previously available data from hybridization of the same microarray platform with other 20 samples (both from the wild-type strain and from a *hetR* mutant strain either in the presence of ammonium or after different periods of nitrogen deprivation) [3] were included in the analysis. The expression data from the 24 samples (Table S1) were analyzed as described [3], and a correlation table was

obtained for NsiR3 (Table S2). The probe with the strongest negative correlation with NsiR3 ( $-0.943$ ) was that of gene *alr0540* (*putA*), encoding proline oxidase. Moreover, another probe corresponding to the 5'-UTR of *alr0540* had a strong negative correlation as well ( $-0.884$ ). Figure 7A shows the expression profile of NsiR3 and *putA* in the 24 samples hybridized to the arrays. We also confirmed by northern blot the opposite

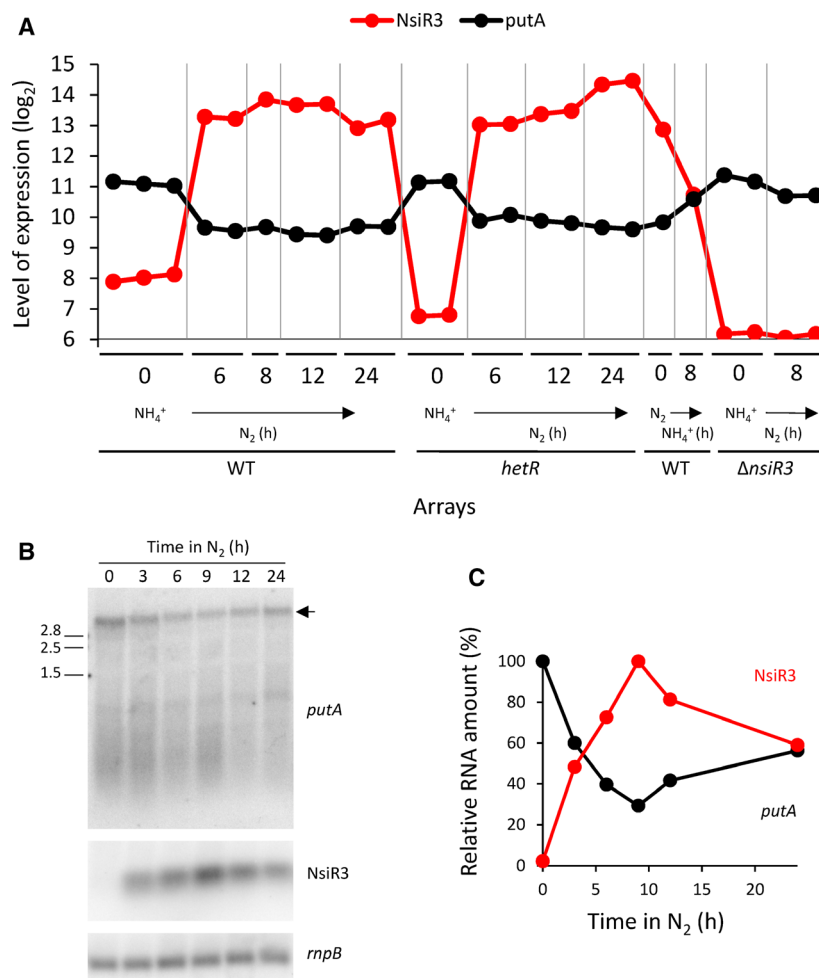


**Fig. 7.** Negative correlation of *putA* and *nsiR3* expression. (A) Expression level of *nsiR3* (red) and *putA* (*alr0540*, black), in the 24 RNA samples hybridized to the microarrays used for the co-expression analysis. (B) *putA* expression after removal of combined nitrogen. RNA was extracted from *Nostoc* cultures at different times after nitrogen removal and subjected to northern blot. The filter was hybridized with probes for *putA* (top), *nsiR3* (middle), and *rnpB* (bottom), that was used as loading control. The experiment was repeated three times with similar results. The northern blot containing the highest number of time points is shown. (C) Quantification of the blot shown in (B). The amount of *putA* mRNA (black) and *NsiR3* (red) is expressed as percentage of the maximum. For *putA*, the full-length transcript (arrow in B) was used in quantification. Sizes of ribosomal RNAs are indicated in (B).

expression dynamics of *putA* with *NsiR3* that was deduced from the co-expression analysis (Fig. 7B).

The results described above strongly suggest that the expression of *putA* might be regulated by *NsiR3*. In fact, we could predict with IntaRNA [25] an interaction between *NsiR3* and the 5'-UTR of *putA* mRNA (Fig. 8A). *NsiR3* would bind to positions  $-5$  to  $-17$  with respect to the initiation codon of *putA*, occluding the ribosome-binding site.

To verify the interaction between *NsiR3* and the 5'-UTR of *putA*, we used a heterologous reporter system [26] in which the 5'-UTR plus the first 60 nt of the *putA* coding sequence was translationally fused to the gene encoding superfolder GFP (*sfgfp*). This construct was co-expressed in *E. coli* either with *NsiR3* or with a control, unrelated RNA. The initiation codon of *putA* was changed from GTG to ATG for optimal expression in *E. coli*. The fluorescence of cells carrying *sfgfp* fusions significantly decreased when *NsiR3* was co-expressed, indicating a negative effect of *NsiR3* on expression of sfGFP (Fig. 8B).

To verify the interactions between *NsiR3* and the mRNA of *putA*, we created a mutated version of *NsiR3* altered in position 14 (G to C, *NsiR3* Mut14) (Fig. 8A). The mutation in *NsiR3* eliminated the interaction between *NsiR3* and the mRNA of *putA* (Fig. 8B). We designed a compensatory mutation in the 5'-UTR of *putA* (Comp-14\*17) that would restore the interaction with *NsiR3* (Mut14) (Fig. 8A). When *NsiR3* (Mut14) was combined with the mutated version of the 5'-UTR of *putA*, the reduction of fluorescence was restored (Fig. 8B). All together, these results verify the interaction of *NsiR3* with the 5'-UTR of *putA* at the positions predicted by IntaRNA. In consequence, an inhibitory effect of *NsiR3* on *putA* in the *in vivo* context of the heterologous *E. coli* system is supported.

### ***NsiR3* represses the expression of *putA* in *Nostoc* sp. PCC 7120**

To analyze the regulatory effect of *NsiR3* on *putA* in *Nostoc* sp. PCC 7120, we generated a *Nostoc* strain



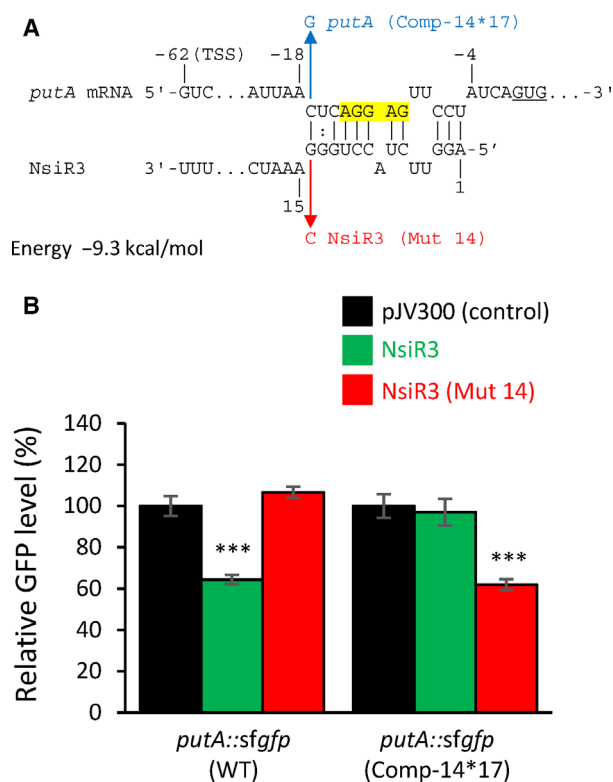


**Fig. 8.** Verification of NsiR3 interaction with the 5'-UTR of *putA* using an *in vivo* reporter system. (A) Predicted interaction between NsiR3 and the 5'-UTR of *putA* mRNA according to INTARNA [25]. Nucleotides are numbered with respect to the start of the coding sequence (initiation codon is underlined). The ribosome-binding site in the *putA* mRNA is highlighted in yellow. A mutation introduced in NsiR3 at position 14 (G to C, Mut14) and the corresponding compensatory mutation in *putA* 5'-UTR position -17 (C to G, Comp-14\*17) are indicated in red and blue, respectively. (B) Fluorescence measurements of *E. coli* DH5 $\alpha$  cultures bearing combinations of plasmids expressing different versions of NsiR3 and *putA::sfgfp* fusions. Plasmid pJV300 (encoding a control RNA) was used as control. The data are presented as the mean  $\pm$  standard deviation of cultures from eight independent colonies after subtraction of fluorescence in cells bearing pXG-0 (\*\*\*)  $P < 0.0001$ , Student *t*-test).

with controlled expression of NsiR3 by complementing strain  $\Delta nsiR3$  with a plasmid containing *nsiR3* under control of the copper-inducible *petE* promoter ( $\Delta nsiR3 + P_{petE}::nsiR3$ ). Accumulation of the mRNA of *putA* was analyzed by northern blot in the wild-type,  $\Delta nsiR3$ , and  $\Delta nsiR3 + P_{petE}::nsiR3$  strains at different times after nitrogen removal and copper addition (Fig. 9A). A stronger reduction in the amount of the full-length *putA* mRNA was observed in the  $\Delta nsiR3 + P_{petE}::nsiR3$  strain than in the wild-type, in agreement with the observation that  $\Delta nsiR3 + P_{petE}::nsiR3$  accumulated about 40 times more NsiR3 than

the wild-type (Fig. 9A,B). The deletion of *nsiR3* in the  $\Delta nsiR3$  strain resulted in levels of the *putA* mRNA that were not significantly reduced after 24 h in the absence of combined nitrogen. These results indicate a strong negative correlation between the amount of NsiR3 and the amount of the *putA* mRNA. As a control, we hybridized the same filter with a probe for gene *agrE* encoding the bifunctional enzyme arginine dihydrolase/ornithine cyclodeaminase that acts upstream proline oxidase in the catabolic pathway from arginine to proline [27]. The dynamic of changes in the amount of *agrE* mRNA upon nitrogen removal was different to that of *putA*. In the wild-type strain, whereas the amount of *putA* mRNA was reduced to about 40% after 24 h in the absence of combined nitrogen, no significant change was observed in the case of *agrE*. In addition, the levels of *agrE* mRNA did not correlated to changes in the amount of NsiR3 (Fig. 9), as predicted for a mRNA that is not a target of NsiR3.

## Discussion

In this work, we characterize NsiR3, a highly conserved sRNA in heterocystous cyanobacteria. NsiR3 was identified in the genomes of seventy heterocyst-forming cyanobacteria but was not found in unicellular or filamentous strains that do not develop heterocysts. This distribution of the *nsiR3* gene, in contrast to that of other NtcA-regulated sRNAs such as NsiR4, also found in unicellular strains [10], suggests a relevant function related to the specific metabolic traits of heterocyst-forming strains. *nsiR3* is not transcribed in the presence of ammonium, but its transcription is strongly induced upon transfer to nitrogen-free medium, suggesting a possible function in the response to nitrogen stress. Furthermore, *nsiR3* transcription is also induced upon transfer from ammonium- to nitrate-containing medium. However, in this case the induction is lower and transient. This can be explained because the nitrogen stress is quickly relieved upon induction of the nitrate assimilation pathway in the presence of nitrate [23]. We show that the global regulator of nitrogen assimilation, NtcA, binds directly to the *nsiR3* promoter, explaining the previous observation that NtcA is required for expression of NsiR3 [9,11]. By means of a fusion to the *gfp* gene, we show that expression of NsiR3, although induced in all cells of the filament under nitrogen deprivation, is much stronger in heterocysts than in vegetative cells. This observation might be explained by the higher concentration of NtcA present in the heterocyst *versus* in vegetative cells [28,29]. Alternatively, the *nsiR3* promoter

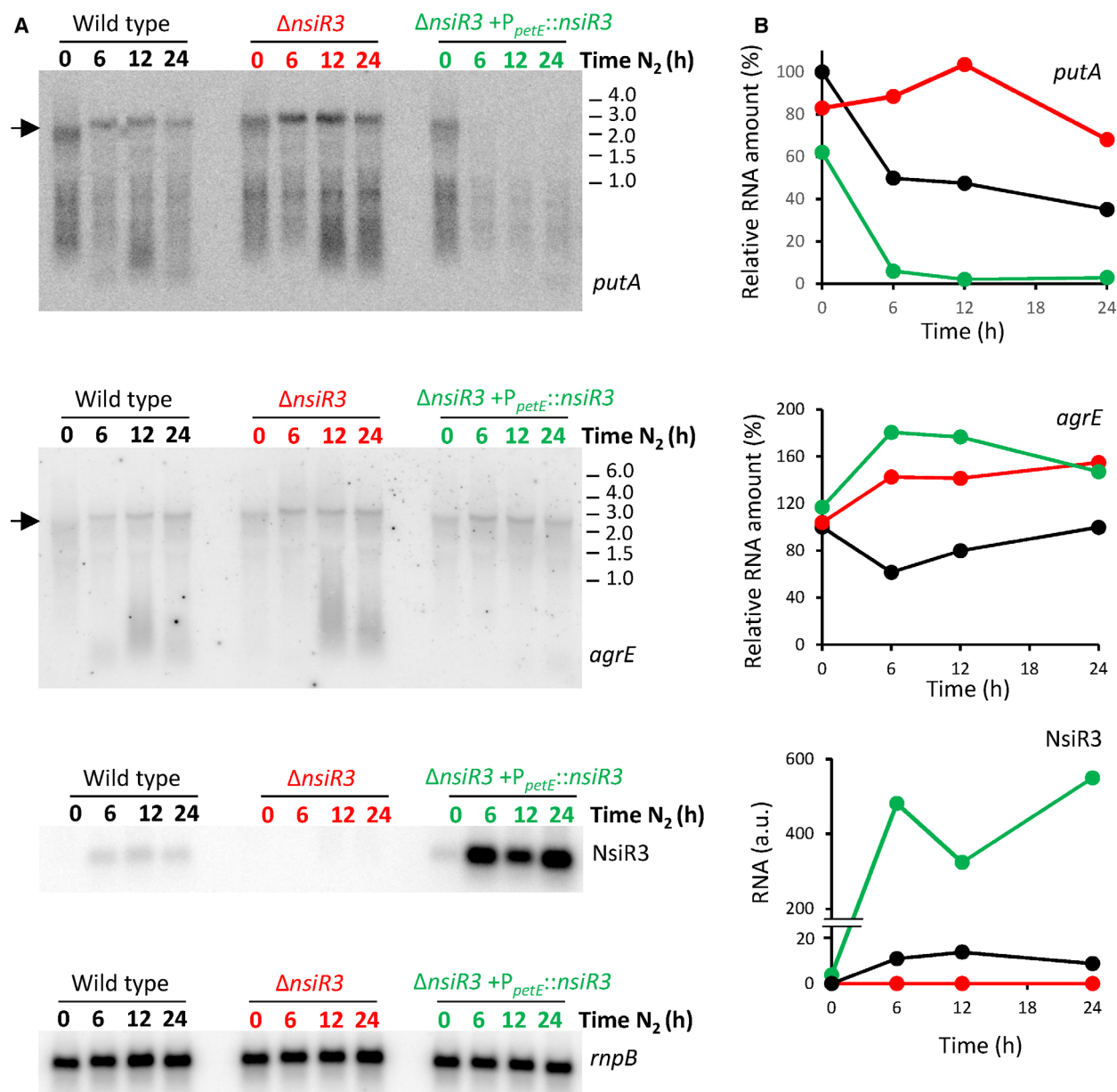


**Fig. 9.** Expression of *putA* and *agrE* in strains with altered levels of NsiR3. (A) Expression was analyzed by northern blot in wild-type, a mutant strain lacking NsiR3 ( $\Delta nsiR3$ ) and in the same strain complemented with a plasmid bearing *nsiR3* under control of the  $\text{Cu}^{2+}$ -regulated promoter of the *petE* gene ( $\Delta nsiR3 + P_{petE}::nsiR3$ ). Cells were grown in the presence of ammonium in medium lacking  $\text{Cu}^{2+}$  (to prevent expression of the *petE* promoter) and transferred to medium containing no source of combined nitrogen ( $\text{N}_2$ ) and  $1.5 \mu\text{M}$   $\text{Cu}^{2+}$  for the indicated number of hours. The filter was hybridized with probes for *putA* (top), *agrE*, *nsiR3*, and *rnpB* (bottom, used as loading control). Size standards are indicated on the right in kb. The experiment was performed twice with similar results. (B) Quantification of the blots shown in (A). The full-length transcripts (arrows in A) were used in quantification. RNA amounts of *putA* and *agrE* mRNAs in wild-type (black),  $\Delta nsiR3$  (red), and  $\Delta nsiR3 + P_{petE}::nsiR3$  (green) strains are expressed relative to the amount present in the wild-type at time 0. NsiR3 amounts are expressed as absolute values.

might contain a response element for an unknown heterocyst-specific factor in addition to the NtcA-binding site. However, neither the DIF1 nor the DIF2 sequence motifs previously described for heterocyst-

specific expression [3,9] are found in the region upstream of the *nsiR3* gene. The observation that a NtcA-regulated RNA, although not exclusively expressed in heterocysts, exhibits differential

expression in this particular cell type suggests the possibility of heterocyst-specific regulation perhaps based on different levels of NtcA and/or 2-oxoglutarate.

One of the main challenges in the study of sRNAs is the identification of their regulated targets. A number of computational and experimental methods have been developed for this purpose [20]. Here, we took advantage of a co-expression analysis, based on hybridization of RNA samples obtained from wild-type, *hetR*, and  $\Delta$ *nsiR3* strains grown under different conditions, to analyze the correlation in expression profiles between *nsiR3* and every gene in *Nostoc* sp. PCC 7120. *putA* (encoding proline oxidase) showed the strongest negative correlation with NsiR3 and was confirmed in this work as a true target of NsiR3 by means of several experimental approaches both in *E. coli* and in *Nostoc*. Co-expression analysis could be a good alternative to identify sRNA targets, provided that enough global data (from microarrays or RNA-Seq) are available to compute the correlation index in expression changes between the sRNA under study and every gene expressed in the organism of interest, as shown here for NsiR3. This was especially relevant in this study because *putA* was not identified as a high-ranking potential candidate target of NsiR3 by predictive computational approaches (not shown). A simple differential expression analysis between wild-type and  $\Delta$ *nsiR3* strain would not allow the identification of *putA* as a potential target of NsiR3 because the fold change (FC) of *putA* mRNA levels between  $\Delta$ *nsiR3* strain and WT after 8 h of nitrogen starvation was not significant enough ( $\log_2$  FC = 0.85) (Table S1). It is relevant to mention that the approach we have used relies on the post-transcriptional regulation by the sRNA on its target having a quantitative impact on the amount of the target mRNA, as is the case for NsiR3 and *putA*.

A *Nostoc* strain lacking NsiR3 ( $\Delta$ *nsiR3*) did not show distinct phenotypic alterations under standard laboratory growth conditions. This is an observation that has been made with null mutants of many other regulatory sRNAs such as NsiR4 [10] or IsaR1 as well [30]. These mutants do not have a distinct phenotype under standard laboratory growth conditions but eventually might reveal phenotypic alterations in a natural environment, where cells are subjected to fluctuating conditions, or the presence of specific substances in the medium, or a combination of factors.

NsiR3 has a clear impact on *putA* expression. In the wild-type strain, the amount of *putA* mRNA was reduced upon nitrogen stress (Figs 7 and 9). However, this reduction was less profound in the  $\Delta$ *nsiR3* mutant (Fig. 9). In contrast, overexpression of NsiR3 from the

*petE* promoter resulted in a strong reduction of *putA* mRNA levels that even became undetectable. We have not studied the molecular mechanism of the post-transcriptional regulation exerted by NsiR3 on *putA* expression. However, the binding site of NsiR3 on the *putA* mRNA overlaps with the predicted ribosome-binding site; therefore, a reasonable assumption is that NsiR3 inhibits the initiation of *putA* translation. A secondary consequence of translation inhibition would be destabilization of the *putA* mRNA, resulting in its degradation. An active mechanism by which NsiR3 recruits an RNase to degrade *putA* mRNA cannot be excluded.

A final question relates to the possible biological relevance of the repression of *putA* upon nitrogen stress. *putA* encodes proline oxidase, a bifunctional enzyme that converts proline to glutamate. Therefore, *putA* is important for proline utilization and also for arginine catabolism that produces proline by the bifunctional enzyme ArgE [27]. Interestingly, *putA* mRNA is not detected in *Nostoc* heterocysts [27]. The higher transcription of NsiR3 in heterocysts (Fig. 5) could result in complete degradation of *putA* mRNA specifically in this cell type and could explain why *putA* is not detected in heterocysts. ArgE is also absent in heterocysts [27]; therefore, the main arginine catabolism pathway is blocked in these cells (Fig. 10), facilitating the channeling of arginine to the biosynthesis of cyanophycin granules that accumulate at high levels in heterocysts and are a source, together with glutamine, of combined nitrogen for vegetative cells (Fig. 10). Modulation of proline oxidase in vegetative cells during diazotrophic growth could also be necessary to avoid excessive glutamate accumulation under conditions in which there is a net gain of glutamate in vegetative cells through glutamine oxoglutarate aminotransferase (GOGAT) acting on glutamine provided by the heterocyst (Fig. 10).

It is unknown if transcriptional regulation is involved in the absence of *putA* mRNA in the heterocyst, but in any case, the expression of NsiR3 at initial stages of heterocyst differentiation could facilitate faster shutdown of *putA* expression than can be achieved by transcriptional regulation only.

NsiR3 adds to a growing number of sRNAs with functions related to nitrogen assimilation in different groups of bacteria, including *E. coli* [31], or *Pseudomonas* [32,33]. In cyanobacteria, several NtcA-regulated sRNAs have been described to regulate responses to nitrogen deficiency, including phycobilisome degradation [12] or glutamine synthetase (GS) activity [10]. Recently, NsiR1, a heterocyst-specific sRNA, has been described to modulate heterocyst differentiation [17].

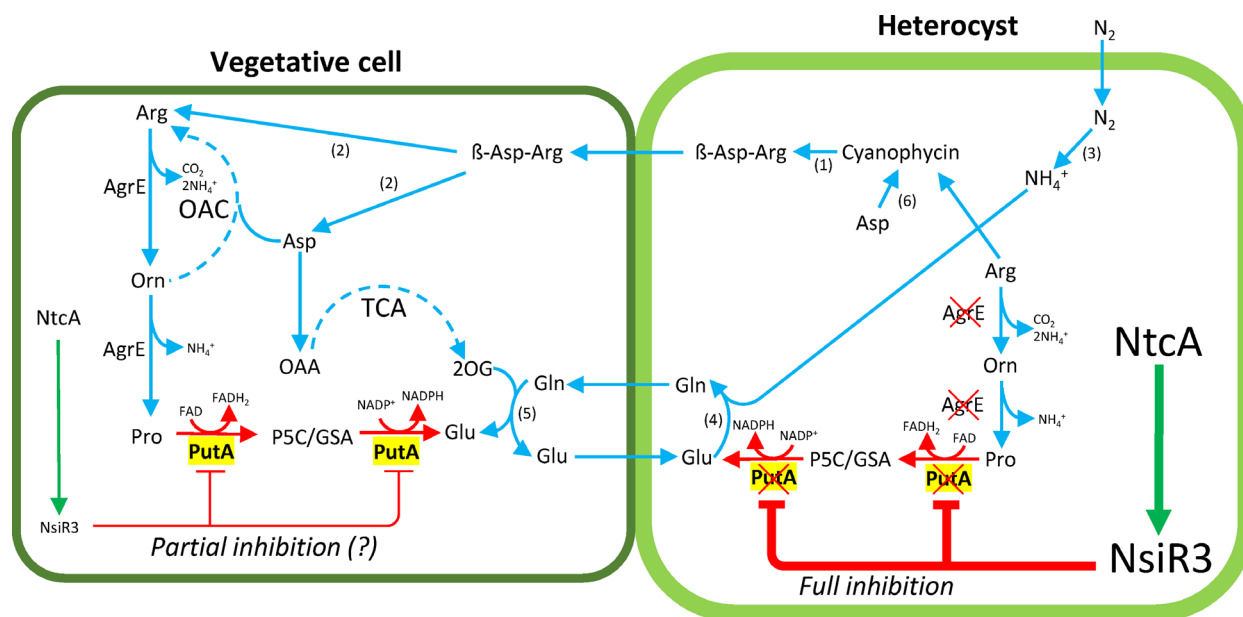


**Fig. 10.** Model of *putA* regulation by NsiR3. Blue arrows represent the most relevant enzymatic reactions in the metabolism of arginine and proline in vegetative cells and heterocysts that are discussed in the text. (1) Cyanophycinase, (2) isoaspartyl dipeptidase, (3) nitrogenase, (4) GS, (5) GOGAT, (6) cyanophycin synthetase, bifunctional arginine dihydrolase/ornithine cyclodeaminase (AgrE), and proline oxidase (PutA). The positive transcriptional regulation of NsiR3 by NtcA is represented by green arrows. NtcA and NsiR3 are more abundant in the heterocyst. Red truncated lines indicate the inhibition of PutA by NsiR3. The red crosses illustrate the absence of AgrE and PutA in heterocysts [27]. The meaning of the abbreviations used is as follows:  $\beta$ -Asp-Arg,  $\beta$ -aspartylarginine; P5C,  $\Delta^1$ -pyrroline-5-carboxylate; GSA, glutamate  $\gamma$ -semialdehyde; 2-OG, 2-oxoglutarate; OAA, oxaloacetate; OAC, ornithine–ammonium cycle; TCA, tricarboxylic acid cycle.

We have previously identified an antisense RNA that shuts down, specifically in heterocyst, the expression of sedoheptulose-1,7-bisphosphatase, a key Calvin cycle enzyme [13]. Here, we describe a trans-acting sRNA that could be relevant for the inhibition of proline oxidase expression specifically in heterocysts, reinforcing the relevance that noncoding RNAs could have in the metabolic adaptations required for heterocyst function. Global analysis [3] suggests that more antisense and sRNA, still to be characterized, could be involved in the heterocyst-specific regulation of key enzymes of the intermediary metabolism. Post-transcriptional RNA regulation could be an important layer of regulation in the metabolic adaptations of heterocysts, together with better known transcriptional regulation that is worth exploring.

## Methods

### Strains and growth conditions

*Nostoc* sp. PCC 7120 wild-type,  $\Delta$ *nsiR3*, and  $\Delta$ *nsiR3*+*P*<sub>petE</sub>:*nsiR3* strains (Table S3) were grown photoautotrophically at

30 °C in BG11 medium [34] containing ferric citrate instead of ammonium ferric citrate. For northern blot analysis of expression under different conditions, cultures of *Nostoc* sp. PCC 7120 were bubbled with an air/CO<sub>2</sub> mixture (1% v/v) and grown photoautotrophically at 30 °C in BG11 medium supplemented with 10 mM NaHCO<sub>3</sub> (BG11C) lacking NaNO<sub>3</sub> but containing 6 mM NH<sub>4</sub>Cl and 12 mM *N*-[Tris (hydroxymethyl)methyl]-2-aminoethanesulfonic acid/NaOH buffer (pH 7.5) (BG11C + NH<sub>4</sub><sup>+</sup>). To induce nitrogen deficiency, filaments were collected by filtration, washed, and resuspended in nitrogen-free BG11 medium containing 10 mM NaHCO<sub>3</sub> (BG11<sub>0</sub>C). To induce the expression of the *petE* promoter, 1.5  $\mu$ M CuSO<sub>4</sub> was added to the cultures at the time of nitrogen removal. To test growth of different strains on plates under different conditions, liquid cultures of these strains growing in BG11 media were diluted to A<sub>750</sub> 0.17 and 10  $\mu$ L of serial fivefold dilutions was spotted on plates containing different nitrogen sources.

*Nostoc* sp. PCC 7120 derivative strains bearing Sm<sup>R</sup>Sp<sup>R</sup> plasmids were grown in the presence of streptomycin (Sm) and spectinomycin (Sp), 2  $\mu$ g·mL<sup>-1</sup> each (liquid medium) or 5  $\mu$ g·mL<sup>-1</sup> each (solid medium).

*E. coli* strains (Table S3) were grown in LB medium, supplemented with appropriate antibiotics [35].

### Electrophoresis mobility shift assay

NtcA was purified as described [12]. Electrophoresis mobility shift assays were carried out as described [36] with a 150-bp PCR fragment amplified with oligonucleotides 23 and 469, encompassing positions –118 to +31 with respect to the TSS of *nsiR3*. A mutated version of the same DNA fragment was obtained by overlap extension PCR using mutagenic complementary oligonucleotides 420 and 421 and flanking oligonucleotides 23 and 469. The DNA fragment was labeled with [ $\gamma$ - $^{32}$ P]ATP and polynucleotide kinase, and 2000–6000 cpm (< 30 pM) were used in each assay.

### Reporter assay for *in vivo* verification of targets

We used the reporter assay described in Ref. [37] and fusions to the gene encoding superfolder GFP (*sfgfp*) in plasmid pXG10-SF [26] for experimental target verification in *E. coli* (Table S4). In this system, both the GFP fusions and NsiR3 are transcribed constitutively.

5'-UTR of *putA* was cloned in pXG10-SF from its TSS, taken from Ref. [9], to 60 nucleotides within the coding region. To facilitate translation in *E. coli*, the GTG start codon of *putA* was replaced by ATG using overlapping PCR and oligonucleotides specified in Table S5. PCR fragments containing the region to be cloned were amplified using genomic DNA as template and oligonucleotides specified in Table S5. Fragments were digested with NsiI and NheI and cloned into pXG10-SF treated with the same enzymes, resulting in translational fusions to sfGFP (Table S6).

To express NsiR3 in *E. coli*, the sequence encoding NsiR3 was amplified from genomic DNA using primers 195 (5' phosphorylated) and 283. The PCR product was digested with XbaI and fused to a plasmid backbone that was amplified from pZE12-luc with primers PLlacOB and PLlacOD [37] and digested with XbaI, rendering pIAE19 (Table S6).

For the mutagenesis of NsiR3 and the 5'-UTR of *putA*, mutations were introduced by overlapping PCR with primers containing the desired changes (Table S5) and the fragments were cloned in the same way as the corresponding wild-type versions.

Combinations of plasmids bearing fragments encoding NsiR3 (or its mutated versions) and the 5'-UTRs of target genes (or mutated versions) were introduced in *E. coli* DH5 $\alpha$ . Plasmid pJV300, expressing an unrelated RNA, was used as a control. Fluorescence measurements were done with a microplate reader (Varioskan) using liquid cultures from eight individual colonies of cells carrying each plasmid combination, as previously described [38].

### Fluorescence microscopy

Plasmid pSAM341, containing the promoter of *nsiR3* fused to *gfpmut2* (Table S4), was introduced in *Nostoc* by conjugation [39] with selection for resistance to Sm and Sp. Images

of filaments containing pSAM341 were taken 4 days after plating in media with ammonium or without combined nitrogen. The accumulation of GFP along the filaments was analyzed and quantified using a Leica (Wetzlar, Alemania) TCS SP2 confocal laser scanning microscope as described [16]. GFP was excited at 488 nm by an argon ion laser, and the fluorescence emission was monitored by collection across windows of 500–538 nm (GFP imaging) and 630–700 nm (cyanobacterial autofluorescence). At least 10 fields of each strain were analyzed. Representative images are shown in Fig. 5. Images were treated with IMAGEJ 1.45 s software (Rasband, W.S., IMAGEJ, U. S. National Institutes of Health, Bethesda, MD, USA, <http://imagej.nih.gov/ij/>, 1997–2018).

### Generation of *Nostoc* strains with altered levels of NsiR3

To generate a strain lacking NsiR3 ( $\Delta$ *nsiR3*), two overlapping fragments encompassing flanking sequences around NsiR3 were amplified by PCR using genomic DNA as template and oligonucleotides 127 and 129 or oligonucleotides 128 and 130, respectively. The resulting products were then used as templates for a third PCR with oligonucleotides 127 and 128, resulting in the fusion of both fragments and the deletion of the sequences encoding NsiR3. The fragment was cloned into pSpark (Canvax Biotech, Córdoba, Spain), rendering pELV16, and its sequence was verified by sequencing. After digestion with BamHI at the sites provided by oligonucleotides 127 and 128, the fragment was cloned into BamHI-digested, *sacB*-containing Sm<sup>R</sup>Sp<sup>R</sup> vector pCSRO [40], rendering pELV17, which was transferred to *Nostoc* sp. PCC 7120 by conjugation [39] with selection for resistance to Sm and Sp. Cultures of the exconjugants obtained were used to select for clones resistant to 5% sucrose [41], and individual sucrose-resistant colonies were checked by PCR. Clones lacking the deleted *nsiR3* region were named  $\Delta$ *nsiR3*.

To establish controlled expression of NsiR3 in *Nostoc*, the *nsiR3* gene was placed under control of the *petE* promoter, which mediates Cu<sup>2+</sup>-regulated transcription [42] and was cloned in a self-replicating plasmid. The *petE* promoter of *Nostoc* sp. PCC 7120 (genomic coordinates 278 185–277 848) was amplified with oligonucleotides 299 and 302 and fused to the *nsiR3* fragment amplified with oligonucleotides 301 and 300 by a third PCR using the two fragments as templates and oligonucleotides 299 and 300. After digestion with ClaI and XhoI at the sites provided by oligonucleotides 299 and 300, the fragment was cloned into pSAM221 [12], rendering pIAE24. pIAE24 was introduced into the  $\Delta$ *nsiR3* strain by conjugation as described above with selection for resistance to Sm and Sp.

### RNA isolation and northern blot analysis

Total RNA was isolated using hot phenol as described [43] with modifications [11]. Northern blot detection of NsiR3

(Fig. 2) was performed using 10% urea–polyacrylamide gels as described [6] and 7.5 µg of total RNA. Northern blot hybridization of mRNAs (Figs 7 and 9) was performed using 1% agarose denaturing formaldehyde gels and 10 µg of total RNA. All RNA samples were then transferred to Hybond-N+ membrane (GE Healthcare, Chicago, IL, USA) with 20× SSC buffer. Strand-specific <sup>32</sup>P-labeled probes were prepared with Taq DNA polymerase using a PCR fragment as template and oligonucleotides specified in Table S5 in a reaction with [ $\alpha$ -<sup>32</sup>P]dCTP and one single oligonucleotide as primer (corresponding to the complementary strand of the sRNA or mRNA to be detected). PCR fragments used as templates for NsiR3, *putA*, and *agrE* probes were amplified from genomic DNA using oligonucleotides pairs 125/126, 645/646, and 909/910, respectively. Hybridization to *rnpB* [44] or 5S rRNA was used as a loading and transfer control for agarose or urea–polyacrylamide gels, respectively.

### Computational methods

Sequences of homologs of NsiR3 were taken from reference [11]. Additionally, NsiR3 sequences were identified by BLAST search of the NCBI genomic database [45]. The prediction of the interaction between NsiR3 and the 5'-UTR of predicted targets in *Nostoc* sp. PCC 7120 was performed using INTARNA [25]. Alignment of NsiR3 homologs was made using CLUSTAL OMEGA [46]. Secondary structure of NsiR3 was predicted by RNAALIFOLD [47].

Processing of microarray data and comparison of expression between samples were performed as described [3]. Raw data were extracted with the read.maimages function of the *limma* R package [48], and the average expression of elements with multiple probes was calculated using the *avereps* function. We performed the following comparisons of expression between two samples to extract differentially expressed probes: every sample *versus* the absolute reference (wild-type 0 h from the -N experiment = ammonium-grown cells), every sample *versus* its own reference (for instance,  $\Delta$ *nsiR3* 8 *versus*  $\Delta$ *nsiR3* 0), and finally sample of the  $\Delta$ *nsiR3* 8 h after nitrogen removal *versus* the wild-type 8 h after nitrogen removal. A total of 6048 genetic elements (genes, putative sRNAs, putative asRNAs, etc.) that exhibited a log<sub>2</sub>FC (fold change) > 1.5 in at least one of the comparisons shown in Table S1 were selected for further analysis. A Pearson correlation analysis was performed between the expression profile of NsiR3 and the expression profile of any other feature (Table S2). The microarray data can be accessed in the GEO database under the accession numbers GSE120377 and GSE150191.

### Acknowledgements

This work was supported by grants BFU2013-48282-C2-1-P from Ministerio de Economía y Competitividad and BFU2016-74943-C2-1-P from Agencia Estatal de Investigación (AEI), Ministerio de Economía, Industria

y Competitividad, both cofinanced by European Regional Development Fund, to AMM-P and by the Federal Ministry of Education and Research (BMBF) program de.NBI-Partner grant 031L0106B to WRH. IÁ-E was the recipient of a predoctoral contract from Ministerio de Economía y Competitividad, Spain (BES-2014-068488). MB-Á was the recipient of a predoctoral contract from Ministerio de Educación, Cultura y Deporte, Spain (FPU2014/05123 and EST16-00088). We thank Alicia Orea (IBVF, CSIC\_Universidad de Sevilla) for technical assistance with microscopy.

### Conflict of interest

The authors declare no conflict of interest.

### Author contributions

AV and AMM-P planned the experiments. IÁ-E, EO-V, AV, and AMM-P performed the experiments. MB-Á, JG, AV, and AMM-P analyzed the data. AV, WRH, and AMM-P wrote the paper.

### References

- Muro-Pastor AM & Hess WR (2012) Heterocyst differentiation: from single mutants to global approaches. *Trends Microbiol* **20**, 548–557.
- Flores E & Herrero A (2010) Compartmentalized function through cell differentiation in filamentous cyanobacteria. *Nat Rev Microbiol* **8**, 39–50.
- Brenes-Álvarez M, Mitschke J, Olmedo-Verd E, Georg J, Hess WR, Vioque A & Muro-Pastor AM (2019) Elements of the heterocyst-specific transcriptome unravelled by co-expression analysis in *Nostoc* sp. PCC 7120. *Environ Microbiol* **21**, 2544–2558.
- Flores E, Picossi S, Valladares A & Herrero A (2019) Transcriptional regulation of development in heterocyst-forming cyanobacteria. *Biochim Biophys Acta Gene Regul Mech* **1862**, 673–684.
- Wagner EGH & Romby P (2015) Small RNAs in bacteria and archaea: who they are, what they do, and how they do it. *Adv Genet* **90**, 133–208.
- Steglich C, Futschik ME, Lindell D, Voss B, Chisholm SW & Hess WR (2008) The challenge of regulation in a minimal photoautotroph: non-coding RNAs in *Prochlorococcus*. *PLoS Genet* **4**, e1000173.
- Flaherty BL, Van Nieuwerburgh F, Head SR & Golden JW (2011) Directional RNA deep sequencing sheds new light on the transcriptional response of *Anabaena* sp. strain PCC 7120 to combined-nitrogen deprivation. *BMC Genomics* **12**, 332.
- Mitschke J, Georg J, Scholz I, Sharma CM, Dienst D, Bantscheff J, Voss B, Steglich C, Wilde A, Vogel J *et al.*

- (2011) An experimentally anchored map of transcriptional start sites in the model cyanobacterium *Synechocystis* sp. PCC6803. *Proc Natl Acad Sci USA* **108**, 2124–2129.
- 9 Mitschke J, Vioque A, Haas F, Hess WR & Muro-Pastor AM (2011) Dynamics of transcriptional start site selection during nitrogen stress-induced cell differentiation in *Anabaena* sp. PCC7120. *Proc Natl Acad Sci USA* **108**, 20130–20135.
  - 10 Klähn S, Schaal C, Georg J, Baumgartner D, Knippen G, Hagemann M, Muro-Pastor AM & Hess WR (2015) The sRNA NsiR4 is involved in nitrogen assimilation control in cyanobacteria by targeting glutamine synthetase inactivating factor IF7. *Proc Natl Acad Sci USA* **112**, E6243–E6252.
  - 11 Brenes-Álvarez M, Olmedo-Verd E, Vioque A & Muro-Pastor AM (2016) Identification of conserved and potentially regulatory small RNAs in heterocystous cyanobacteria. *Front Microbiol* **7**, 48.
  - 12 Álvarez-Escribano I, Vioque A & Muro-Pastor AM (2018) NsrR1, a nitrogen stress-repressed sRNA, contributes to the regulation of *nblA* in *Nostoc* sp. PCC 7120. *Front Microbiol* **9**, 2267.
  - 13 Olmedo-Verd E, Brenes-Álvarez M, Vioque A & Muro-Pastor AM (2019) A heterocyst-specific antisense RNA contributes to metabolic reprogramming in *Nostoc* sp. PCC 7120. *Plant Cell Physiol* **60**, 1646–1655.
  - 14 Muro-Pastor AM & Hess WR (2020) Regulatory RNA at the crossroads of carbon and nitrogen metabolism in photosynthetic cyanobacteria. *Biochim Biophys Acta Gene Regul Mech* **1863**, 194477.
  - 15 Ionescu D, Voss B, Oren A, Hess WR & Muro-Pastor AM (2010) Heterocyst-specific transcription of NsiR1, a non-coding RNA encoded in a tandem array of direct repeats in cyanobacteria. *J Mol Biol* **398**, 177–188.
  - 16 Muro-Pastor AM (2014) The heterocyst-specific NsiR1 small RNA is an early marker of cell differentiation in cyanobacterial filaments. *MBio* **5**, e01079-14.
  - 17 Brenes-Álvarez M, Minguet M, Vioque A & Muro-Pastor AM (2020) NsiR1, a small RNA with multiple copies, modulates heterocyst differentiation in the cyanobacterium *Nostoc* sp. PCC 7120. *Environ Microbiol* **22**, 3325–3338.
  - 18 Backofen R & Hess WR (2010) Computational prediction of sRNAs and their targets in bacteria. *RNA Biol* **7**, 33–42.
  - 19 Barquist L & Vogel J (2015) Accelerating discovery and functional analysis of small RNAs with new technologies. *Annu Rev Genet* **49**, 367–394.
  - 20 Georg J, Lalaouna D, Hou S, Lott SC, Caldelari I, Marzi S, Hess WR & Romby P (2020) The power of cooperation: experimental and computational approaches in the functional characterization of bacterial sRNAs. *Mol Microbiol* **113**, 603–612.
  - 21 Mazel D, Houmard J, Castets AM & Tandeau de Marsac N (1990) Highly repetitive DNA sequences in cyanobacterial genomes. *J Bacteriol* **172**, 2755–2761.
  - 22 Vioque A (1997) The RNase P RNA from cyanobacteria: short tandemly repeated repetitive (STRR) sequences are present within the RNase P RNA gene in heterocyst-forming cyanobacteria. *Nucleic Acids Res* **25**, 3471–3477.
  - 23 Cai Y & Wolk CP (1997) Nitrogen deprivation of *Anabaena* sp. strain PCC 7120 elicits rapid activation of a gene cluster that is essential for uptake and utilization of nitrate. *J Bacteriol* **179**, 258–266.
  - 24 Herrero A & Flores E (2019) Genetic responses to carbon and nitrogen availability in *Anabaena*. *Environ Microbiol* **21**, 1–17.
  - 25 Mann M, Wright PR & Backofen R (2017) IntaRNA 2.0: enhanced and customizable prediction of RNA-RNA interactions. *Nucleic Acids Res* **45**, W435–W439.
  - 26 Corcoran CP, Podkaminski D, Pappenfort K, Urban JH, Hinton JCD & Vogel J (2012) Superfolder GFP reporters validate diverse new mRNA targets of the classic porin regulator, MicF RNA. *Mol Microbiol* **84**, 428–445.
  - 27 Burnat M, Picossi S, Valladares A, Herrero A & Flores E (2019) Catabolic pathway of arginine in *Anabaena* involves a novel bifunctional enzyme that produces proline from arginine. *Mol Microbiol* **111**, 883–897.
  - 28 Olmedo-Verd E, Muro-Pastor AM, Flores E & Herrero A (2006) Localized induction of the *ntcA* regulatory gene in developing heterocysts of *Anabaena* sp. strain PCC 7120. *J Bacteriol* **188**, 6694–6699.
  - 29 Sandh G, Ramström M & Stensjö K (2014) Analysis of the early heterocyst Cys-proteome in the multicellular cyanobacterium *Nostoc punctiforme* reveals novel insights into the division of labor within diazotrophic filaments. *BMC Genom* **15**, 1064.
  - 30 Georg J, Kostova G, Vuorijoki L, Schön V, Kadowaki T, Huokko T, Baumgartner D, Müller M, Klähn S, Allahverdiyeva Y *et al.* (2017) Acclimation of oxygenic photosynthesis to iron starvation is controlled by the sRNA IsaR1. *Curr Biol* **27**, 1425–1436.e7.
  - 31 Wang C, Chao Y, Matera G, Gao Q & Vogel J (2020) The conserved 3' UTR-derived small RNA NarS mediates mRNA crossregulation during nitrate respiration. *Nucleic Acids Res* **48**, 2126–2143.
  - 32 Wenner N, Maes A, Cotado-Sampayo M & Lapouge K (2014) NrsZ: a novel, processed, nitrogen-dependent, small non-coding RNA that regulates *Pseudomonas aeruginosa* PAO1 virulence. *Environ Microbiol* **16**, 1053–1068.
  - 33 Zhan Y, Yan Y, Deng Z, Chen M, Lu W, Lu C, Shang L, Yang Z, Zhang W, Wang W *et al.* (2016) The novel regulatory ncRNA, NfiS, optimizes nitrogen fixation via base pairing with the nitrogenase gene *nifK* mRNA in

- Pseudomonas stutzeri* A1501. *Proc Natl Acad Sci USA* **113**, E4348–E4356.
- 34 Rippka R, Deruelles J, Waterbury JB, Herdman M & Stanier RY (1979) Generic assignments, strain histories and properties of pure cultures of cyanobacteria. *Microbiology* **111**, 1–61.
- 35 Sambrook J & Russell DW (2001) *Molecular Cloning: A Laboratory Manual*. Cold Spring Harbor Laboratory, Cold Spring Harbor, NY.
- 36 Muro-Pastor AM, Valladares A, Flores E & Herrero A (1999) The *hetC* gene is a direct target of the NtcA transcriptional regulator in cyanobacterial heterocyst development. *J Bacteriol* **181**, 6664–6669.
- 37 Urban JH & Vogel J (2007) Translational control and target recognition by *Escherichia coli* small RNAs *in vivo*. *Nucleic Acids Res* **35**, 1018–1037.
- 38 Wright PR, Richter AS, Papenfort K, Mann M, Vogel J, Hess WR, Backofen R & Georg J (2013) Comparative genomics boosts target prediction for bacterial small RNAs. *Proc Natl Acad Sci USA* **110**, E3487–E3496.
- 39 Elhai J & Wolk CP (1988) Conjugal transfer of DNA to cyanobacteria. *Methods Enzymol* **167**, 747–754.
- 40 Merino-Puerto V, Mariscal V, Mullineaux CW, Herrero A & Flores E (2010) Fra proteins influencing filament integrity, diazotrophy and localization of septal protein SepJ in the heterocyst-forming cyanobacterium *Anabaena* sp. *Mol Microbiol* **75**, 1159–1170.
- 41 Cai Y & Wolk CP (1990) Use of a conditionally lethal gene in *Anabaena* sp. strain PCC 7120 to select for double recombinants and to entrap insertion sequences. *J Bacteriol* **172**, 3138–3145.
- 42 Buikema WJ & Haselkorn R (2001) Expression of the *Anabaena hetR* gene from a copper-regulated promoter leads to heterocyst differentiation under repressing conditions. *Proc Natl Acad Sci USA* **98**, 2729–2734.
- 43 Mohamed A & Jansson C (1989) Influence of light on accumulation of photosynthesis-specific transcripts in the cyanobacterium *Synechocystis* 6803. *Plant Mol Biol* **13**, 693–700.
- 44 Vioque A (1992) Analysis of the gene encoding the RNA subunit of ribonuclease P from cyanobacteria. *Nucleic Acids Res* **20**, 6331–6337.
- 45 Altschul SF, Gish W, Miller W, Myers EW & Lipman DJ (1990) Basic local alignment search tool. *J Mol Biol* **215**, 403–410.
- 46 Madeira F, Park YM, Lee J, Buso N, Gur T, Madhusoodanan N, Basutkar P, Tivey ARN, Potter SC, Finn RD *et al.* (2019) The EMBL-EBI search and sequence analysis tools APIs in 2019. *Nucleic Acids Res* **47**, W636–W641.
- 47 Lorenz R, Bernhart SH, Höner zu Siederdissen C, Tafer H, Flamm C, Stadler PF & Hofacker IL (2011) ViennaRNA package 2.0. *Algorithms Mol Biol* **6**, 26.
- 48 Ritchie ME, Phipson B, Wu D, Hu Y, Law CW, Shi W & Smyth GK (2015) limma powers differential expression analyses for RNA-sequencing and microarray studies. *Nucleic Acids Res* **43**, e47.
- 49 Crooks GE, Hon G, Chandonia J-M & Brenner SE (2004) WebLogo: a sequence logo generator. *Genome Res* **14**, 1188–1190.
- 50 Voss B, Bolhuis H, Fewer DP, Kopf M, Möke F, Haas F, El-Shehawey R, Hayes P, Bergman B, Sivonen K *et al.* (2013) Insights into the physiology and ecology of the brackish-water-adapted Cyanobacterium *Nodularia spumigena* CCY9414 based on a genome-transcriptome analysis. *PLoS One* **8**, e60224.

## Supporting information

Additional supporting information may be found online in the Supporting Information section at the end of the article.

**Table S1.** Differentially\_expressed\_genes\_all\_samples.

**Table S2.** Pearson\_correlation\_of\_NsiR3\_and\_all\_genes.

**Table S3.** Strains.

**Table S4.** Plasmids.

**Table S5.** Oligonucleotides.

**Table S6.** Sequences.